

Feasibility Analysis of On-Orbit Debris Detection Using Commercial Star Trackers

Allan Shtofenmakher^{a,*}, Hamsa Balakrishnan^a

^a*Department of Aeronautics and Astronautics, Massachusetts Institute of Technology, Cambridge, Massachusetts, USA*

Abstract

The U.S. Space Surveillance Network (SSN) currently tracks over 23,000 resident space objects (RSOs) in low-earth orbit (LEO). The SSN uses ground-based radar and optical methods, which are susceptible to variations in atmosphere, weather, and lighting conditions. These barriers limit the surveillance capabilities to objects with characteristic length greater than 10 cm. Consequently, hundreds of thousands of smaller RSOs in LEO remain untracked, reducing overall space situational awareness. Prior research has demonstrated the feasibility of using space-based commercial star trackers (CSTs) to detect and track objects larger than 10 cm in characteristic length. The analysis we present in this paper shows that CSTs can also be used to detect debris particles below 10 cm in size.

We model particles as Lambertian spheres with zero phase angle and ten percent reflectivity. The apparent visual magnitude of debris particles is expressed as a function of particle size and RSO-CST distance and compared against the sensitivity levels of a variety of CSTs. We find that, when properly illuminated, debris of characteristic length between 1 cm and 10 cm can be detected by some CSTs even at distances of tens of kilometers. More sensitive CSTs can characterize RSOs at the larger end of this scale (i.e., 10 cm) hundreds of kilometers away; alternatively, they can track objects smaller than 1 cm at closer distances.

Keywords: Space Situational Awareness (SSA); Orbital Debris Detection; Satellite-Based Optical Sensors; Small Orbital Debris; Apparent Visual Brightness

1. Introduction and Background

As the number of resident space objects (RSOs) in low Earth orbit (LEO) grows, the risk of collision between RSOs increases dramatically, threatening the sustainability of space as a resource [1]. The U.S. Space Surveillance Network (SSN) currently tracks over 23,000 RSOs in LEO, including functional and decommissioned satellites and debris [2]. However, the ground-based radar and optical methods used by the SSN are susceptible to variations in atmosphere, weather, and lighting conditions [3]. Due to these barriers, the focus of ground-based surveillance methods is often restricted to objects larger than 10 cm in characteristic length [2]. This leaves hundreds of thousands of smaller RSOs in LEO larger than 1 cm but smaller than 10 cm in characteristic length that are untracked by ground-based methods [2]. The associated reduction in space situational awareness (SSA) has contributed to incidents such as the recent Soyuz MS-22 coolant leak on the International Space Station, which is suspected to have been caused by a 1-mm-scale RSO and rendered the spacecraft unsafe for return flight [4, 5]. Improved strategies for detecting and tracking the space debris population are therefore necessary to mitigate the risk of compromising civil, commercial, and defense satellite applications in LEO.

Prior research has proposed the use of onboard satellite sensors to detect and track RSOs. Space-based sensors are often more sensitive than their ground-based counterparts and can therefore detect smaller and dimmer objects [3]. Among such space-based sensors, the commercial star tracker (CST) is a promising choice because of its low cost (relative to other space-based RSO sensors) and its widespread deployment on active satellites [6]. The CST is an

*Corresponding author

Email addresses: ashtofen@mit.edu (Allan Shtofenmakher), hamsa@mit.edu (Hamsa Balakrishnan)

optical sensor that captures images of distant stars and compares them to onboard star catalogs to determine spacecraft attitude [6]. In addition to stars, incidental RSOs that are illuminated by sunlight and are in line of sight of the CST are also often captured in these images [6].

Recent work has therefore assessed the feasibility of using CSTs to observe, detect, and estimate the position and velocity of RSOs, with a focus on meter-scale and larger satellites. For example, [6] and [7] explore the details of observing and detecting RSOs of this size using one or multiple CSTs, while [8] and [9] explore various methods for estimating the positions and velocities of such RSOs. [10] evaluates the performance of one such approach, finding that the accuracy of RSO position estimates is on par with or superior to the accuracy levels identified in [11] for ground-based tracking. However, most prior work has focused on RSOs with characteristic length greater than 10 cm, with the goal of improving position and velocity knowledge of those objects that are already tracked using ground-based methods.

In this paper, we explore the feasibility of using CSTs to detect sub-10-cm-class articles of debris. In Sec. 2, we derive a simple mathematical relationship among AVM, RSO size, and RSO-CST distance. Despite its simplicity, this relationship provides insight into the parameter space (in terms of debris size and distance) that can feasibly be detected by CSTs. We discuss the key findings of this analysis in Sec. 3. We conclude with some directions for further analysis and research in Sec. 4.

2. Theory and Methodology

2.1. Apparent Visual Magnitude Calculation

This section introduces a mathematical relationship among an RSO’s AVM, optical cross section (OCS), and distance from CST. The ability of a CST to observe an RSO depends on the RSO’s AVM, as determined by the satellite observer. The AVM of an RSO in LEO, V_{rso} , can be expressed as a function of the RSO-CST distance, R , the object’s optical cross section, A_{opt} , and the AVM of the Sun at Earth, V_{sun} [12]:

$$V_{\text{rso}} = V_{\text{sun}} - \frac{5}{2} \log_{10} \frac{A_{\text{opt}}}{R^2} \quad (1)$$

More *negative* values of AVM correspond to *brighter* objects. In particular, in the equation above, the Sun has an AVM at Earth of roughly $V_{\text{sun}} = -26.5$ [13]. At any given time, an object’s OCS is a function of geometric and material properties and angle relative to the Sun. To assess detection feasibility, [13] devised a conservative method for estimating mean OCS, using time-averaged, ground-based AVM and distance measurements from [14] as inputs to Eqn. 1. This method requires the observed object to be illuminated by the Sun and in line of sight of the observer. Since [14]’s measurements were performed from the ground, the results are estimated to be conservative by up to 1 AVM unit [13].

Table 1 below presents [13]’s mean OCS (i.e., A_{opt}) estimates for two spacecraft (SpinSat and DMSP-5D2 F7) and further applies the same methodology to another spacecraft (POPACS) using additional mean AVM and distance data from [14]. With A_{opt} determined, Eqn. 1 yields a semi-logarithmic relationship between AVM and RSO-CST distance for each spacecraft, which is visualized in Sec. 3.1. The POPACS spacecraft in particular serves as a useful baseline because of its 10-cm spherical shape.

Spacecraft	Char. Length (cm)	Mean Orbit Alt. (km)	Sun AVM	Mean AVM	Mean OCS (m ² /sr)
POPACS NanoSat [14]	10	838	-26.5	12	0.00028
SpinSat [13]	56	345	-26.5	9	0.00075
DMSP-5D2 F7 [13]	930	835	-26.5	7	0.02776

Table 1: Mean OCS values for several representative spacecraft. Adapted from [13] using data from [14].

2.2. Diffuse Lambertian Sphere Model

Since ground-based AVM data is only available for a small subset of RSOs, a standard model for OCS must be leveraged for articles of debris. According to [15], the Inter-Agency Space Debris Coordination Committee (IADC) defines a standard method for modeling debris in optical debris campaigns. In particular, debris particles are modeled as diffuse Lambertian spheres with zero phase angle and ten percent reflectivity.

The original form of Eqn. 1 is attributed to Barker (2004) for optical measurements of near-Earth objects illuminated by the Sun [15]. In the Barker (2004) model, the optical cross section of a Lambertian sphere is expressed as a function of the reflectivity or albedo, ρ , of the surface, the diameter, d , of the sphere, and the phase function, $F(\phi)$, for the given phase angle, ϕ , as follows [15]:

$$A_{\text{opt}} = \frac{1}{4}\pi d^2 \rho F(\phi) \quad (2)$$

According to [16], the phase function for such an object is given by:

$$F(\phi) = \frac{2}{3\pi^2}[(\pi - \phi) \cos(\phi) + \sin(\phi)] \quad (3)$$

Moreover, when the phase angle is zero, the phase function becomes:

$$F(0) = \frac{2}{3\pi} \quad (4)$$

Combining Eqns. 1, 2, and 3 with the IADC standard model offers a relationship among debris diameter, RSO-CST distance, and AVM:

$$V_{\text{rso}} = V_{\text{sun}} - \frac{5}{2} \log_{10} \frac{d^2}{60R^2} \quad (5)$$

With this simplified model, it is possible to determine the AVM of any debris particle of a given size at a given distance, and, consequently, whether that particle can be detected by a given CST.

2.3. CST Sensor Limits

A variety of star tracker (ST) categories and their representative performance specifications are described in [17]. Included among these qualities is the AVM cutoff—the limiting magnitude of an object that can be detected by a ST for a given signal-to-noise ratio (SNR) and exposure time. Table 2 below presents AVM cutoff and other supplementary information for several representative ST classes. The front-illuminated (FI) CST represents a typical microsatellite-class ST, while the high-precision (HP) CST corresponds to a relatively high-end optical sensor, and the nano CST offers properties typical of a space-constrained, CubeSat-class star tracker.

CST Type	Example	Exposure Time (s)	SNR (dB)	AVM Cutoff
HP CST/Imager	MOST Space Telescope [18]	0.1	11	11.1
FI CST	BOKZ-MF	0.1	15	6.5
Nano CST	Berlin Space Technologies ST200	0.1	7	4.8

Table 2: Selected properties of representative CSTs/imagers. Adapted from [17] unless otherwise stated.

As sensing technology is continuously improving, the results in Table 2 can be considered conservative with respect to the capabilities of the latest generation of CSTs. These representative CST AVM limits are represented graphically in Sec. 3 to denote the boundary at which RSOs of a given size and at a given distance can still be detected.

3. Results and Discussion

3.1. Detection Feasibility vs. Distance, Parameterized Across Debris Size

The results of Eqn. 5, using distance as the input variable, are plotted in Fig. 1 for debris of 1 cm and 10 cm in diameter, in gray and black, respectively. For comparison and to serve as baseline, the results of Eqn. 1 for the three spacecraft from Table 1 are also plotted in Fig. 1 as dotted lines. Consistent with Eqn. 5, these curves appear as straight lines when plotted on a semi-log scale. In addition, the AVM cutoff value for each imager listed in Table 2 is presented as a horizontal line for reference.

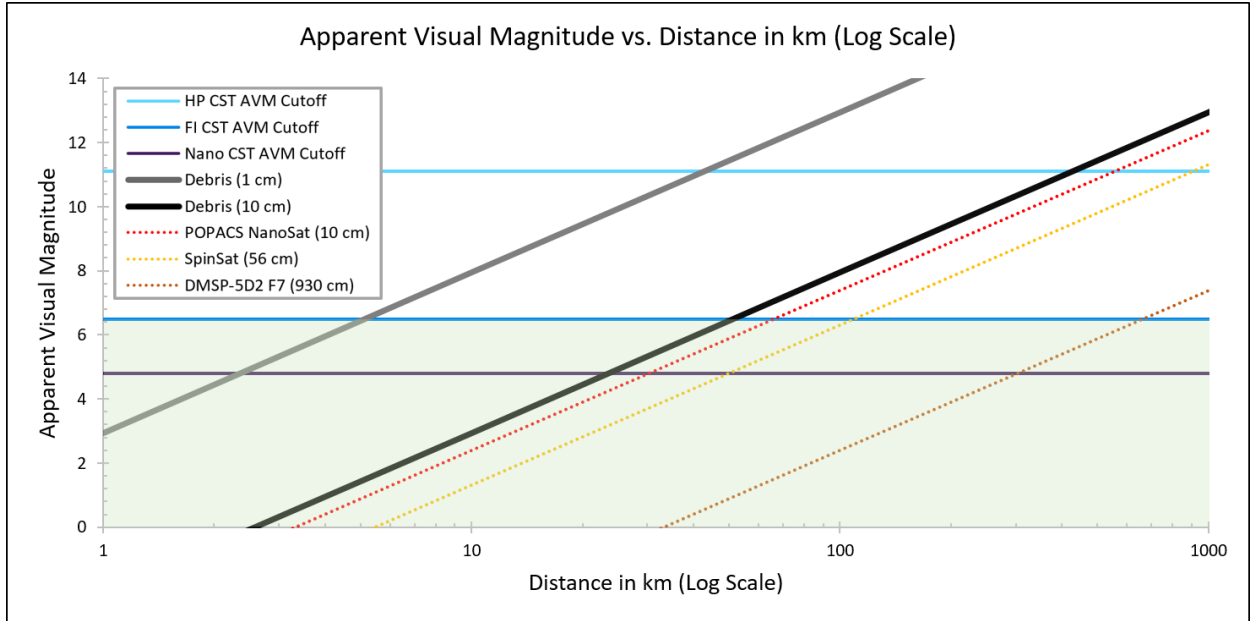


Figure 1: AVM vs. distance between RSO and CST, for representative RSOs of different characteristic lengths. The thin horizontal lines correspond to various sensor AVM cutoffs, while the shaded green region represents the regime which can be detected by typical CSTs. Plots for SpinSat and DMSP-5D2 F7 (adapted from [13]) and for POPACS (using data from [14]) are shown as dotted lines for comparison.

Comparing the results for 10-cm debris and POPACS, debris roughly 10 cm in diameter appears to be only slightly dimmer than a 10-cm diameter nanosatellite under comparable conditions. This corresponds to a reflectivity coefficient of roughly 0.2 for the nanosatellite, which is consistent with the information presented in [19].

From Fig. 1, it is clear that many typical CSTs can be used to detect debris with characteristic length less than 10 cm at distances as far as roughly 50 km. These same sensors have the potential to detect debris as small as 1 cm in diameter as far as 5 km away. Even space-limited CubeSats using nanosatellite-class CSTs can detect 10-cm-class debris at roughly 25 km away or 1-cm-class debris at a distance of 2.5 km. Higher-performing imagers like the MOST telescope can further characterize orbital debris of 10 cm diameter as far as 400 km away or be used to characterize orbital debris smaller than 1 cm at ranges not exceeding 40 km.

Brighter and larger objects such as other satellites can be characterized by these CSTs at distances on the order of hundreds or thousands of kilometers, depending on RSO size and reflectivity, as evidenced by the dotted lines corresponding to the three satellites from Table 1.

3.2. Detection Feasibility vs. Debris Diameter, Parameterized Across Distance

The results of Eqn. 5, using debris diameter as the input variable, are plotted in Fig. 2 across three different RSO-CST ranges (1 km, 10 km, and 100 km). As before, the AVM cutoff value for each imager listed in Table 2 is also shown as a horizontal line. Dotted vertical lines represent the plots for SpinSat (56 cm) and POPACS (10 cm). DMSP-5D2 F7 (930 cm) does not appear in Fig. 2 for scaling reasons. It is worth noting that increasing the RSO-CST range by an order of magnitude increases the AVM (i.e., makes dimmer) of a particular debris particle by 5 units,

which is consistent with expectations from Eqn. 5. This is comparable to the difference between the AVM cutoff values for the HP CST and the FI CST, suggesting that high-performance imagers can generally detect debris an order of magnitude farther away than more typical CSTs.

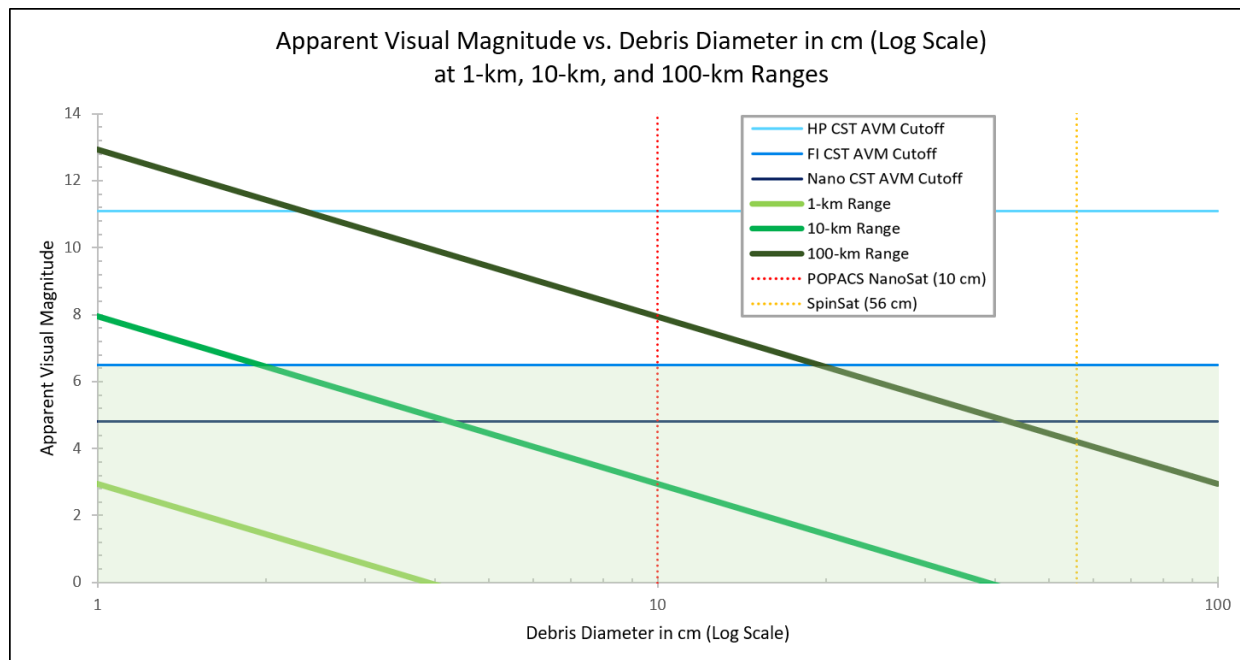


Figure 2: AVM vs. debris diameter for various RSO-CST ranges, assuming diffuse Lambertian spheres in accordance with IADC standards [15]. The thin horizontal lines correspond to various sensor AVM cutoffs, while the shaded green region represents the regime which can be detected by typical CSTs. Plots for SpinSat (adapted from [13]) and for POPACS (using data from [14]) are shown as vertical dotted lines for comparison.

The intersections of the horizontal AVM cutoff lines in Fig. 2 with the thick range lines offers insights into the smallest debris particle that can be detected by each imaging sensor at a given range. In broad terms, the results indicate that all three CST classes depicted should be able to detect debris as small as 1 cm at the relatively close range of 1 km and debris larger than 42.5 cm at the relatively far distance of 100 km.

In theory, based on AVM alone, HP STs are able to detect debris of diameter as small as 2.5 cm at distances as far as 100 km, and debris smaller than 1 cm in diameter at closer distances. The more typical FI STs can detect debris of diameter as small as 2.0 cm at distances as far as 10 km, while nanosatellite-class CSTs can detect 4.0-cm debris at the same distance. Further investigation is needed to determine if—and to what extent—other sensor properties may affect these results in practice.

4. Conclusions and Future Work

In this paper, we presented analysis that suggests that CSTs can be used to detect orbital debris particles between 1 cm and 10 cm in diameter. The debris particles were modeled as diffuse Lambertian spheres in accordance with IADC standards. The AVM of the particles was computed according to the Barker (2004) model for optical measurements of near-Earth objects illuminated by the Sun. Using these models, we determined the AVM of debris particles as a function of particle size and RSO-CST range. These results were compared to the sensitivity levels of several representative imaging sensors to determine the smallest debris size (given range) and farthest distance (given debris diameter) at which detection of the debris particle is feasible.

The results indicate that typical microsatellite-class CSTs can detect illuminated sub-10-cm-class debris particles at ranges as far as tens of kilometers, while higher-performing imagers can characterize illuminated debris as far as hundreds of kilometers. These ranges increase further for larger and brighter RSOs, especially satellites with high reflectivity values. The distance at which a particular CST is able to detect a particular article of debris depends on

many factors, but CSTs designed for precision-pointing applications will generally outperform lower-cost CSTs for micro and nanosatellites. The results also indicate the potential for CSTs and other imagers to be useful in detecting and tracking particles smaller than 1 cm in diameter. However, at such small characteristic lengths, it is anticipated that other imager qualities may reduce the feasibility or usefulness of this approach. For example, the effect of the diffraction limit on the ability of a CST to distinguish between two debris particles at such small sizes requires further investigation. Finally, real debris particles are not typically Lambertian spheres observed at zero phase angle, as assumed in this analysis. Relaxing these assumptions may yield higher-fidelity results.

Now that we have demonstrated the feasibility of using CSTs for space-based detection of debris smaller than 10 cm in characteristic length, we may begin to investigate the various applications of this approach, such as the tracking of small-scale RSOs. In particular, methods that leverage the growing network of CSTs in space are a promising topic for future research.

5. Declaration of Conflicting Interests

The authors declare that they have no conflict of interest with regards to the present research or its publication.

6. Funding

This research was sponsored in part by the United States AFRL and the United States Air Force Artificial Intelligence Accelerator and was accomplished under Cooperative Agreement Number FA8750-19-2-1000. The views and conclusions contained in this document are those of the authors and should not be interpreted as representing the official policies, either expressed or implied, of the United States Air Force or the U.S. Government. The U.S. Government is authorized to reproduce and distribute reprints for Government purposes notwithstanding any copyright notion herein. Allan Shtofenmakher was also supported in part by the Graduate Fellowship for STEM Diversity and the National Institute of Standards and Technology.

7. Authors' Contributions

Allan Shtofenmakher was responsible for conducting the analysis and writing the manuscript. Hamsa Balakrishnan provided necessary guidance and helped with editing.

Acknowledgments

The authors would like to thank Sydney Dolan and Victor Qin for technical discussions and feedback.

References

- [1] R. Hiles, A. Alexander, N. Herzer, D. McKissock, A. Mitchell, J. Sapinoso, [Report on 2020 mega-constellation deployments and impacts to space domain awareness](#), in: Advanced Maui Optical and Space Surveillance Technologies Conference, Maui, HI, 2021. URL <https://amostech.com/TechnicalPapers/2021/SSA-SDA/Hiles.pdf>
- [2] K. L. Hobbs, A. R. Collins, E. M. Feron, [Towards a taxonomy for automatic and autonomous cooperative spacecraft maneuvering in a space traffic management framework](#), in: AIAA ASCEND, 2020. URL <https://doi.org/10.2514/6.2020-4240>
- [3] B. Lal, A. Balakrishnan, B. M. Caldwell, R. S. Buenconsejo, S. A. Carioscia, [Global trends in space situational awareness \(SSA\) and space traffic management \(STM\)](#), Tech. Rep. D-9074, Log H 18-000179, Institute for Defense Analyses Science and Technology Policy Institute, Washington, DC (April 2018). URL <https://apps.dtic.mil/sti/pdfs/AD1123106.pdf>
- [4] E. Howell, Russia's 'final decision' on leaky soyuz spacecraft at space station to come in january: reports, <https://www.space.com/russia-leaky-soyuz-decision-january-2023>, accessed: 2023-12-15 (December 2022).
- [5] B. Tingley, Russia releases 1st images of damage to leaky soyuz spacecraft (photos), <https://www.space.com/soyuz-spacecraft-leak-photos-russia-space-agency>, accessed: 2023-12-15 (February 2023).
- [6] M. Liu, H. Wang, H. Yi, Y. Xue, D. Wen, F. Wang, Y. Shen, Y. Pan, [Space debris detection and positioning technology based on multiple star trackers](#), Applied Sciences 12 (7) (April 2022). URL <https://doi.org/10.3390/app12073593>

- [7] S. Clemens, R. Lee, P. Harrison, W. Soh, [Feasibility of using commercial star trackers for on-orbit resident space object detection](#), in: Advanced Maui Optical and Space Surveillance Technologies Conference, Maui, HI, 2018.
URL https://amostech.com/TechnicalPapers/2018/Space-Based_Assets/Clemens.pdf
- [8] S. Dave, R. Clark, G. Chianelli, R. Lee, [Machine learning implementation for in-orbit RSO orbit estimation using star tracker cameras](#), in: Advanced Maui Optical and Space Surveillance Technologies Conference, Maui, HI, 2022.
URL <https://amostech.com/TechnicalPapers/2020/Machine-Learning-Applications-of-SSA/Dave.pdf>
- [9] S. Dave, R. Lee, [RSO position and velocity estimation using convolutional neural networks from in-orbit star tracker images](#), in: 43rd Committee on Space Research Scientific Assembly, 2021.
- [10] R. Clark, Y. Fu, S. Dave, R. Lee, [Simulation of RSO images for space situation awareness \(SSA\) using parallel processing](#), *Sensors* 21 (23) (November 2021).
URL <https://doi.org/10.3390/s21237868>
- [11] K. Riesing, K. Cahoy, [Orbit determination from two line element sets of ISS-deployed CubeSats](#), in: 29th Annual AIAA/USU Conference on Small Satellites, Logan, UT, 2015.
URL <https://digitalcommons.usu.edu/cgi/viewcontent.cgi?article=3222&context=smallsat>
- [12] J. T. McGraw, M. R. Ackermann, P. C. Zimmer, J. B. Martin, [Blind search for micro satellites in LEO: Optical signatures and search strategies](#), in: Advanced Maui Optical and Space Surveillance Technologies Conference, Maui, HI, 2003.
- [13] M. Driedger, P. Ferguson, [Feasibility study of an orbital navigation filter using resident space object observations](#), *Journal of Guidance, Control, and Dynamics* 44 (3) (2020) 622–628.
URL <https://doi.org/10.2514/1.6005210>
- [14] F. Gasdia, [Optical tracking and spectral characterization of cubesats for operational missions](#), Master's thesis, Embry-Riddle Aeronautical University, Daytona Beach, FL (May 2016).
URL <https://commons.erau.edu/edt/212>
- [15] J. Africano, P. Kervin, D. Hall, P. Sydney, J. Ross, T. Payne, S. Gregory, K. Jorgensen, K. Jarvis, T. Parr-Thumm, G. Stansbery, E. Barker, [Understanding photometric phase angle corrections](#), in: Proceedings of the Fourth European Conference on Space Debris, Darmstadt, Germany, 2005, pp. 141–146.
URL <https://articles.adsabs.harvard.edu/pdf/2005spde.conf..141A>
- [16] J. G. Williams, G. A. McCue, [An analysis of satellite optical characteristics data](#), *Planetary and Space Science* 14 (9) (1966) 839–847.
URL [https://doi.org/10.1016/0032-0633\(66\)90090-0](https://doi.org/10.1016/0032-0633(66)90090-0)
- [17] A. I. Zakharov, M. E. Prokhorov, M. S. Tuchin, A. O. Zhukov, [Minimum star tracker specifications required to achieve a given attitude accuracy](#), *Astrophysical Bulletin* 68 (4) (2013) 481–493.
URL <https://doi.org/10.1134/S199034131304010X>
- [18] S. Rucinski, K. Carroll, R. Kuschnig, J. Matthews, P. Stibrany, [MOST \(Microvariability & Oscillations of Stars\) Canadian astronomical micro-satellite](#), *Advances in Space Research* 31 (2) (2003) 371–373.
URL [https://doi.org/10.1016/S0273-1177\(02\)00628-2](https://doi.org/10.1016/S0273-1177(02)00628-2)
- [19] P. W. Kervin, J. L. Africano, P. F. Sydney, D. Hall, [Small satellite characterization technologies applied to orbital debris](#), *Advances in Space Research* 35 (7) (2005) 1214–1225.
URL <https://doi.org/10.1016/j.asr.2004.11.038>